

Peroxyesters As Precursors to Peroxyl Radical Clocks

Jason J. Hanthorn[†] and Derek A. Pratt^{*,†,‡}

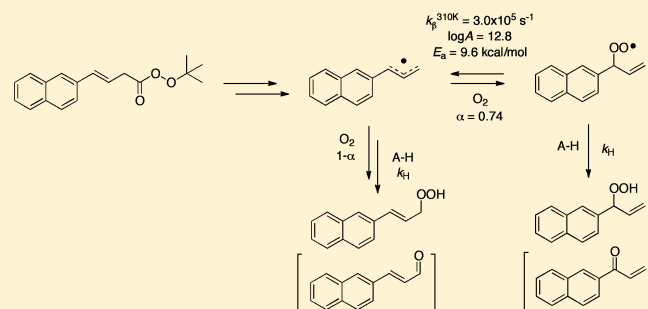
[†]Department of Chemistry, Queen's University, 90 Bader Lane, Kingston, K7L 3N6 Canada

[‡]Department of Chemistry, University of Ottawa, 10 Marie Curie, Ottawa, K1N 6N5 Canada

Supporting Information

ABSTRACT: The reactions of peroxy radicals are at the center of the oxidative degradation of essentially all petroleum-derived hydrocarbons and biological lipids and consequently, the inhibition of these processes by radical-trapping antioxidants. Recently described peroxy radical clocks offer a simple, convenient, and inexpensive method of determining rate constants for H-atom transfer reactions to peroxy radicals, greatly enabling the kinetic and mechanistic characterization of compounds with antioxidant properties. We follow up our preliminary communication on the development of a methodology utilizing *tert*-butyl styrylperacetate as a precursor to a

versatile peroxy radical clock with the present paper, wherein we describe a novel naphthyl analogue, which provides for much improved product resolution for analysis, and provide the complete details associated with its development and application. Using this new precursor, and with consideration of the expanded set of reaction products, inhibition rate constants were measured for a variety of representative phenolic and diarylamine radical-trapping antioxidants. We also provide details for the use of this methodology for the determination of mechanistic information, such as kinetic solvent effects, Arrhenius parameters, and kinetic isotope effects.



INTRODUCTION

Peroxy radicals are the key intermediates in the radical-mediated oxidative degradation (autoxidation) of all organic materials, including primary petroleum products, polymers, foodstuffs, and biological molecules.^{1–3} To slow the rate of autoxidation, radical-trapping antioxidants (e.g., phenols and aromatic amines) are employed industrially (e.g., BHT and 4,4'-dialkyldiphenylamines) and in nature (e.g., α -tocopherol, the most potent form of vitamin E) to “trap” peroxy radicals as hydroperoxides to prevent radical-chain propagation.^{4–6} These compounds donate a hydrogen atom to a chain-carrying peroxy radical, forming a hydroperoxide and a more stable/persistent (i.e., less reactive) antioxidant-derived radical at a rate dependent on antioxidant structure and reaction medium.⁷ Understanding the kinetics of H-atom transfer from antioxidants to peroxy radicals provides important mechanistic information about structure–activity relationships relevant to radical-trapping antioxidants. Several methods have been developed for measuring inhibition rate constants, including inhibited autoxidation, laser flash photolysis and pulse radiolysis. However, these methods all suffer the drawback of requiring specialized equipment and expertise to obtain reliable kinetic data, and they are often limited in the time domain and solvents in which they can be carried out.

Recently, Porter and co-workers⁸ introduced a peroxy radical clock approach based on the kinetic competition between the unimolecular β -fragmentation of a nonconjugated peroxy radical (e.g., **1** derived from allylbenzene as in Scheme 1) and its trapping in a bimolecular reaction with an antioxidant

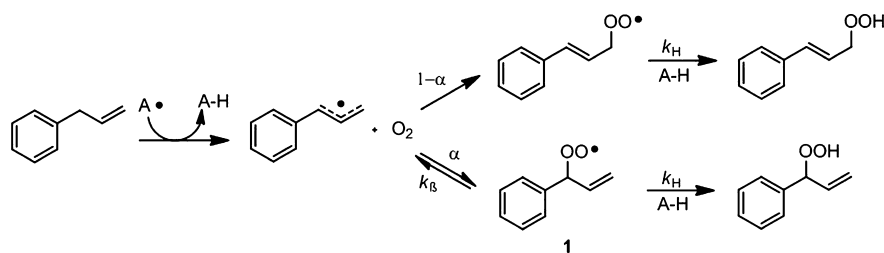
A–H. This methodology requires no specialized equipment other than a GC or HPLC for product analysis. Although the approach is effective for measuring rates of H-atom transfer from many phenols to peroxy radicals in benzene, a major limitation of this method is that it requires the antioxidant-derived radical (A·) to abstract a hydrogen atom from allylbenzene to propagate the chain reaction. This becomes problematic if the antioxidant gives rise to either persistent (e.g., BHT) or highly stabilized (e.g., 6-amino-3-pyridinols)¹⁷ radicals that cannot efficiently propagate the chain. To offset low propagation rate constants, even for the most ideal A–H, a high concentration of oxidizable substrate (e.g., 2.3 M allylbenzene) must be used to ensure enough oxidation products are formed for reproducible analysis. A consequence of using such high concentrations of oxidizable substrate is that it precludes accurate kinetic or mechanistic studies in any solvent other than benzene.

To address the limitations associated with this approach, we recently described the use of the homoconjugated peroxyester **2**⁹ as a precursor to the same delocalized allylbenzene-derived radical essential for the kinetic competition experiment. In our preliminary report, we showed that compound **2** decomposes under aerobic conditions either “thermally” (37 °C) or photolytically (300 nm) to generate nonconjugated peroxy radical **1**, permitting clock experiments using as little as 10 mM of compound **2**. Furthermore, the rate constant for β -fragmentation (k_β) of **1** was measured in a variety of organic solvents, which subsequently

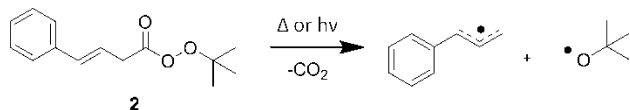
Received: September 12, 2011

Published: November 3, 2011

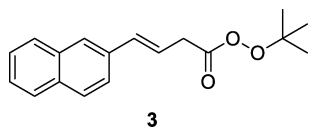
Scheme 1



allowed for the measurement of kinetic solvent effects on the rates of H-atom transfer from phenolic antioxidants.



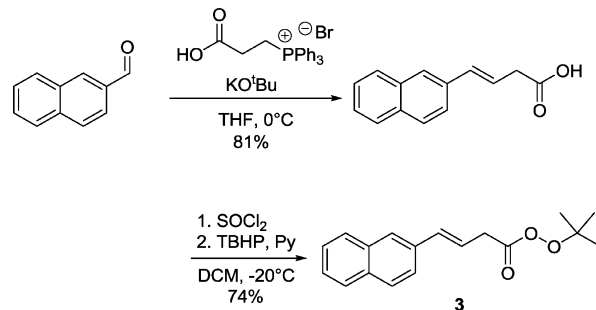
Although the peroxyester approach was successful in obtaining both inhibition rate constants (k_{inh} in Scheme 1) and the effect of solvent upon them for several phenolic antioxidants, one of the aspects we sought to improve prior to any further development or application of the approach was the resolution of the product alcohols (the hydroperoxides are reduced with PPh_3 for analysis by gas chromatography with flame ionization detection), which often had poorly resolved peaks and/or peaks with similar retention times to common phenolic antioxidants and their derivatives. Herein, we describe a second generation peroxy radical clock, derived from the naphthyl-based peroxyester **3**, which yields greatly improved chromatographic resolution and revealed previously unidentified products in the region of the conjugated and nonconjugated alcohols. The origin of these products and their contribution to the accurate measurement of inhibition rate constants using this approach was explored, as well as the role played by the antioxidants in their formation. To demonstrate the utility of the peroxyester approach beyond simple phenolic compounds, we use compound **3** to measure inhibition rate constants for some highly reactive pyrimidinols, pyridinols, and diarylamines. Furthermore, we use **3** to measure deuterium kinetic isotope effects (DKIEs) for a variety of phenolic antioxidants and are able to provide Arrhenius parameters for the β -fragmentation of the nonconjugated peroxy radical derived from **3**, such that it may be applied in the future to study the temperature dependence of inhibition reactions.



RESULTS

I. Synthesis of Peroxyester **3 and its Derived Products.** Synthesis of the acid precursor to (*E*)-*tert*-butyl 4-(naphthalen-2-yl)but-3-eneperoxyacetate **3** was achieved via a Wittig reaction between commercially available 2-naphthaldehyde and the phosphonium salt derived from 3-bromopropionic acid. Subsequent formation of the acid chloride and substitution with *tert*-butyl hydroperoxide afforded the product in 60% yield over the three steps. Upon its preparation, isolation and purification, the first advantage of peroxyester **3** over the analogous phenyl compound **2** was evident: its higher crystallinity enabled easy recrystallization and resulted in

material of higher purity that gave rise to a long shelf life at ambient temperatures.



The corresponding nonconjugated (**4**) and conjugated (**6**) alcohol products used as GC standards for kinetic analysis were also synthesized from 2-naphthaldehyde. Compound **4** was prepared via a Grignard reaction with vinylmagnesium bromide, and compound **6** via a Horner–Wadsworth–Emmons reaction followed by DIBAL reduction of the resulting ester.

Although the conjugated and nonconjugated alcohols were the only products observed in the use of peroxyester **2**,⁹ we observed additional peaks in the same region as the corresponding alcohols **4** and **6** in our calibration experiments with peroxyester **3** with α -tocopherol (vide infra). GC–MS studies indicated they were the corresponding higher oxidized products, ketone **5** and aldehyde **7**, seemingly derived from dehydration of the nonconjugated and conjugated hydroperoxides, respectively. Therefore, we prepared authentic standards of these compounds as well. The nonconjugated ketone **5** was prepared by CrO_3 /*tert*-butyl hydroperoxide oxidation of alcohol **4**, and the conjugated aldehyde **7** via PCC oxidation of alcohol **6** (Scheme 2).

II. Calibration of Peroxy Radical Clock Derived From **3.** In order to “calibrate” the radical clock derived from **3** (determination of k_{β}), we decomposed **3** in the presence of various concentrations of α -tocopherol (α -TOH, **8**) at 37 °C. The resulting hydroperoxides were reduced to their corresponding alcohols with PPh_3 , and the products were analyzed by GC-FID. Examples of gas chromatograms obtained at high and low concentrations of α -TOH are shown in Figure 1. The resulting ratios of nonconjugated/conjugated products were plotted vs $[\alpha\text{-TOH}]$ and the non-linear relationship fit to the equation shown in Figure 2 to determine the rate constant for β -fragmentation of the nonconjugated peroxy radical in a given solvent (Table 1). Values for k_{inh} used to determine k_{β} were obtained by laser flash photolysis for the reaction of α -TOH with cumylperoxy radicals in several different solvents.¹⁰

III. Representative Clocking Experiments Using Peroxyester **3.** To confirm the accuracy of the peroxy radical clock methodology utilizing **3**, k_{inh} values were determined in chlorobenzene for a representative set of antioxidants having

Scheme 2

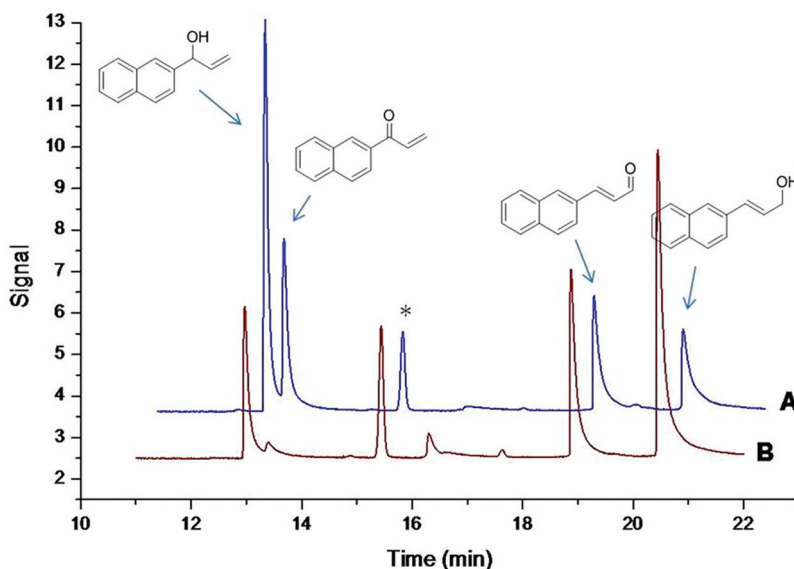
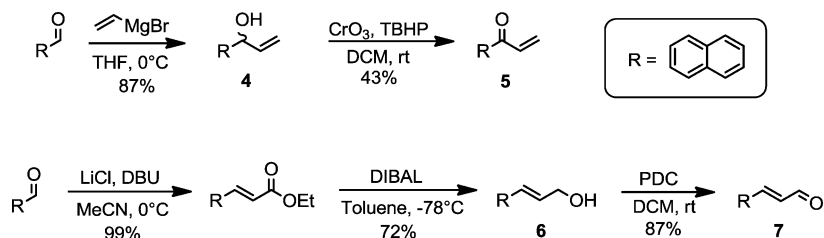


Figure 1. Representative gas chromatograms (GC-FID) in the retention time range of product elution following the incubation of peroxyester **3** with 1.0 M α -TOH (A) and 0.03 M α -TOH (B) for 12 h at 37 °C in chlorobenzene. The peak labeled * is observed in most chromatograms and could not be identified; however, the peak area does not change with antioxidant concentration and therefore appears not to be relevant in our kinetic analysis.

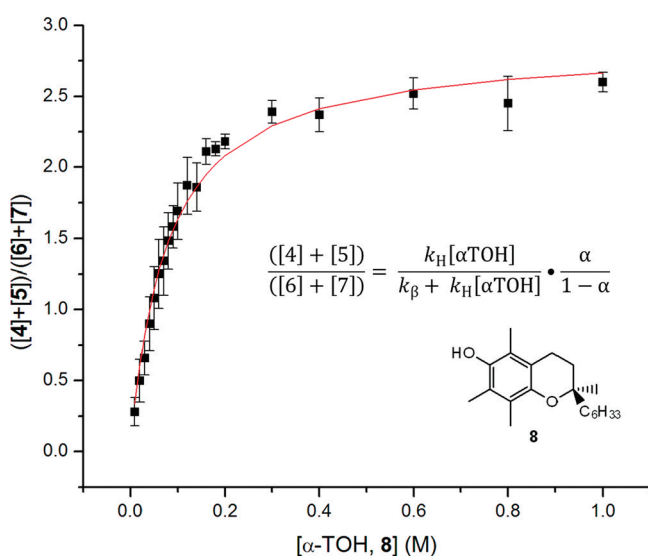


Figure 2. Ratio of nonconjugated ($[4] + [5]$) to conjugated ($[6] + [7]$) oxidation products formed in the decomposition of **3** as a function of $[\alpha\text{-TOH}, \mathbf{8}]$ following incubation for 12 h at 37 °C in benzene.

varied structure and reactivity: 2,4,6-trimethylphenol (**9**), 2,6-di-*tert*-butyl-4-methoxyphenol (**10**), diphenylamine (**11**), phenothiazine (**12**), a pyrimidinol (**13**), and a pyridinol (**14**). The values were obtained simply by decomposing **3** in the presence

Table 1. β -Fragmentation Rate Constants and Oxygen Partition Coefficients of the Nonconjugated Peroxyl Radical Derived from **3** as a Function of Solvent^a

solvent	k_β (s ⁻¹) ^b	α ^c	k_{inh} (M ⁻¹ s ⁻¹) ^d
hexanes	$1.6 (\pm 0.2) \times 10^6$	0.65	2.1×10^7
chlorobenzene	$5.7 (\pm 0.3) \times 10^5$	0.79	7.1×10^6 ^e
benzene	$3.0 (\pm 0.9) \times 10^5$	0.74	3.9×10^6
anisole	$1.9 (\pm 0.5) \times 10^5$	0.69	1.8×10^6
benzonitrile	$1.4 (\pm 0.1) \times 10^5$	0.78	4.7×10^5 ^f
ethyl acetate	$9.5 (\pm 0.3) \times 10^4$	0.76	2.9×10^5
acetic acid	$5.1 (\pm 0.2) \times 10^4$	0.57	1.0×10^6
propionitrile	$2.8 (\pm 0.1) \times 10^4$	0.65	4.7×10^5 ^f

^aInhibition rate constants used in the determination of k_β and α are given for reference. ^bFrom decomposition of **3** at 37 °C. ^cValues are dimensionless and have errors of ± 0.01 . ^dDetermined directly by laser flash photolysis in the given solvent at 25 °C¹⁰ and corrected to 37 °C using $\log A = 8$ and $E_a = 1.6$ kcal/mol, see text. ^eSee ref 11. ^fValue determined in acetonitrile, which has the same β_2^H value (0.45).¹²

of varying amounts of the antioxidant and plotting the ratio of nonconjugated to conjugated products as a function of antioxidant concentration as in Figure 3. The inhibition rate constants determined in this way are shown in Table 2 and are in good-to-excellent agreement with literature values obtained by the inhibited autoxidation of styrene.

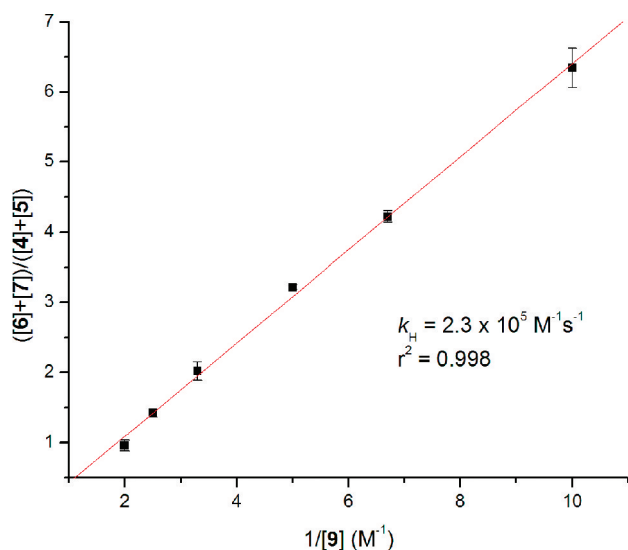
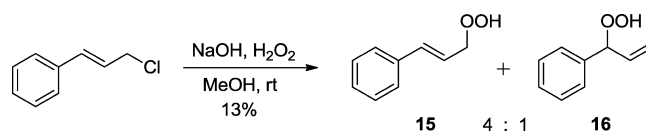


Figure 3. Representative double-reciprocal plot used to obtain inhibition rate constants. Shown is data obtained for 2,4,6-trimethylphenol (**9**) in chlorobenzene at 37 °C.

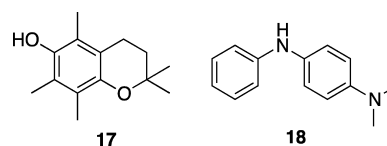
IV. Origin of Carbonyl-Containing Products. Authentic conjugated and nonconjugated hydroperoxides were prepared in order to probe the conditions under which they could serve as a source for the carbonyl products observed when phenothiazine **12**, pyrimidinol **13**, or pyridinol **14** were clocked or when the clock was calibrated with α -TOH in polar media. Bloodworth et al. have reported that cinnamyl-derived hydroperoxides can be prepared from the corresponding cinnamyl chloride by reaction with excess hydrogen peroxide and NaOH, albeit in low yield (11%) as an inseparable mixture of isomers (conjugated/nonconjugated).¹⁸ When the analogous (*E*)-2-(3-chloroprop-1-enyl)naphthalene was subjected to the same conditions in a number of different solvents, the desired hydroperoxides were not isolated, likely because of the solubility of the starting material under these conditions. Therefore, we decided to study the reactivity of the cinnamyl-derived products, given that their reactivity should be essentially the same as their naphthyl analogues. Following the literature procedure, we were able to isolate the cinnamyl-derived hydroperoxides as a 4:1 mixture of conjugated (**15**) and nonconjugated (**16**) hydroperoxides.

To test the stability of the hydroperoxides under the conditions of the clocking experiment, the mixture of isomers



15 and **16** were incubated at 37 °C for 14 h in chlorobenzene or acetonitrile. The mixture was then reduced with PPh₃ and analyzed by GC. The product analysis showed only alcohols **4** and **6** in the same 4:1 ratio observed when the hydroperoxide mixture was reduced with PPh₃ and analyzed immediately. Next, the hydroperoxides were incubated at 37 °C for 14 h in chlorobenzene or acetonitrile containing either **10**, **11**, 2,2,5,7,8-pentamethyl-6-chromanol (a truncated version of α -tocopherol, **17**), or *N*¹,*N*¹-dimethyl-*N*⁴-phenylbenzene-1,4-diamine (**18**) over 14 h at different concentrations. Representative chromatograms are shown in Figure 4.

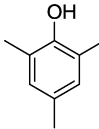
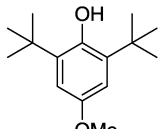
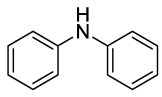
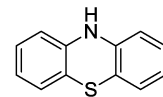
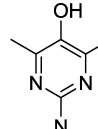
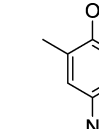
Importantly, although there was a difference in the product composition (alcohols and carbonyls) as a function of antioxidant



structure and solvent, there was no significant change in the 4:1 ratio of conjugated/nonconjugated alcohol + carbonyl products. While it would appear that the hydroperoxide products persist in the presence of the phenols **10** and **17** and the diarylamine **11**, they dehydrate to carbonyls in the presence of more basic diarylamines, such as **18**.¹⁹ Furthermore, the yield of carbonyl products increases upon changing the solvent from chlorobenzene to acetonitrile (see the Supporting Information). In fact, in acetonitrile, carbonyl products are now also observed for phenol **17**.

V. Temperature Dependence of β -Fragmentation. To estimate Arrhenius parameters for the β -fragmentation of the nonconjugated peroxy radical, **3** was decomposed in the presence of varying concentrations (0.02–1.0 M) of α -tocopherol (α -TOH, **8**) at six additional temperatures (45, 50, 60, 70, 80, and 95 °C) in chlorobenzene. Values for k_{inh} used to determine k_{β} at these temperatures were estimated on the basis of $k_{\text{inh}} = 6.4 \times 10^6 \text{ M}^{-1} \text{ s}^{-1}$ in chlorobenzene at 25 °C and $\log A = 8$ (an estimated value, vide infra). The resulting Arrhenius plot is shown in Figure 5, whose slope and intercept yield $E_a = 9.6 (\pm 0.9) \text{ kcal/mol}$ and $\log A = 12.8 (\pm 0.6)$.

Table 2. Rate Constants for Reactions of **9**–**14** with Peroxyl Radicals Generated from Peroxyester **3** at 37 °C in Chlorobenzene^a

compound	clock k_{inh} ($\text{M}^{-1} \text{ s}^{-1}$)	lit k_{inh} ($\text{M}^{-1} \text{ s}^{-1}$)	<i>T</i> , ref
	$2.3 (\pm 0.1) \times 10^5$	8.5×10^4	30 °C, 13
	$5.6 (\pm 1.7) \times 10^5$	1.1×10^5	30 °C, 13
	$4.6 (\pm 0.5) \times 10^4$	4.4×10^4	65 °C, 14
	$8.5 (\pm 0.6) \times 10^6$	8.8×10^6	50 °C, 15
	$1.7 (\pm 2.5) \times 10^7$	8.6×10^{6b}	50 °C, 16
	$3.2 (\pm 1.1) \times 10^7$	1.6×10^7	30 °C, 17

^aLiterature values obtained by inhibited autoxidation of styrene at the given temperatures are shown for comparison. ^bIn benzene.

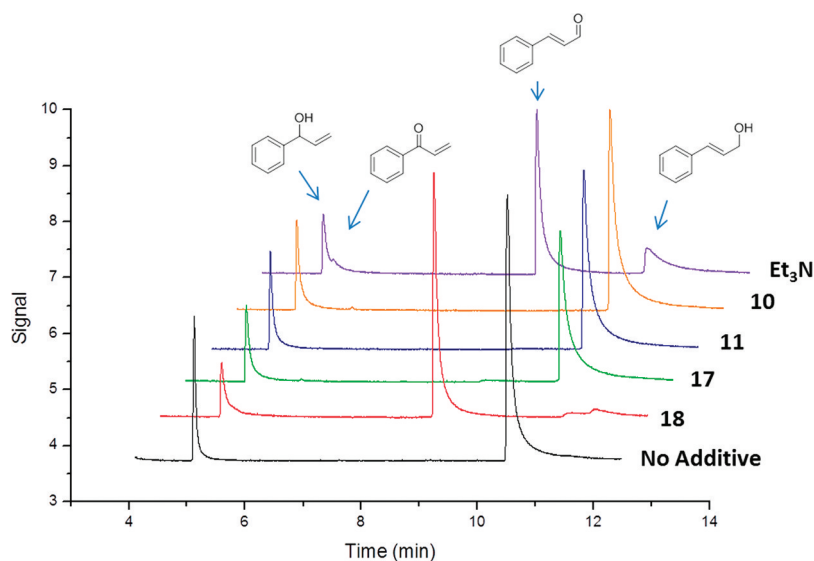


Figure 4. Stacked plot of gas chromatograms (GC-FID) showing product distribution (4, 5, 6, and 7 with R = Ph) arising from hydroperoxide decomposition (5 mM) in the presence of various additives (50 mM) incubated at 37 °C in chlorobenzene. Initial ratio of conjugated/nonconjugated products (15/16) was 4:1.

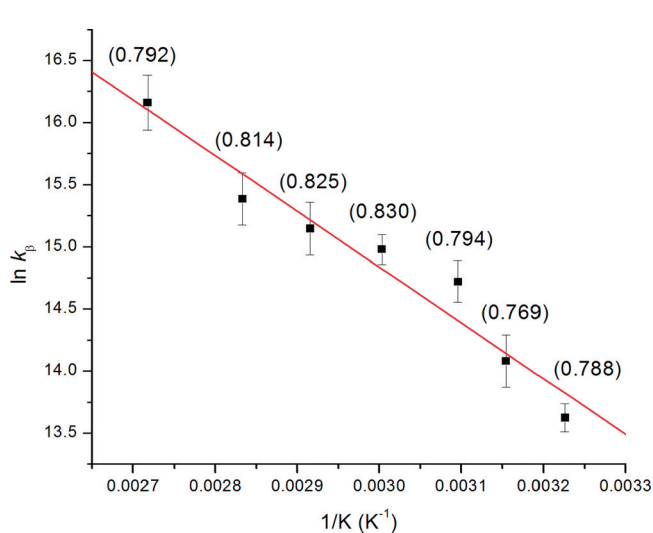


Figure 5. Temperature dependence of the β -fragmentation of the nonconjugated peroxy radical derived from 3, which yields $E_a = 9.6$ (± 0.9) kcal/mol and $\log A = 12.8$ (± 0.6). Corresponding oxygen partition coefficients (α) for each temperature are given in parentheses next to each data point.

VI. Kinetic Isotope Effect Measurements. Deuterium kinetic isotope effects (DKIEs) were measured for a representative set of phenolic antioxidants using the peroxy radical clock methodology. Prior to each experiment, the antioxidant was stirred with an excess (typically 1–5%) of D_2O (and an equivalent amount of H_2O in a parallel experiment as a control).²⁰ Furthermore, the experiment was carried out in the presence of 1% D_2O to ensure adventitious water in the solvent did not shift the equilibrium. A representative plot is shown in Figure 6 for 2,2,5,7,8-pentamethyl-6-chromanol (17), and the DKIEs for it and the other four phenols we examined are summarized in Table 3. For comparison, DKIE values were also measured using the methyl linoleate clock of Porter and co-workers⁸ and are reported alongside.

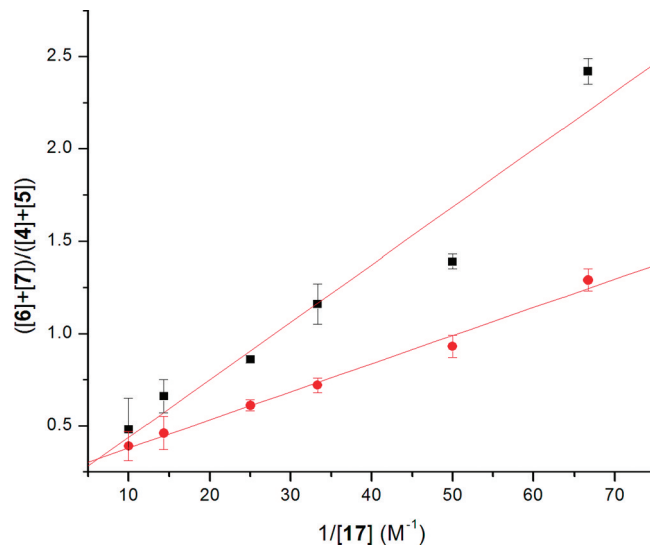


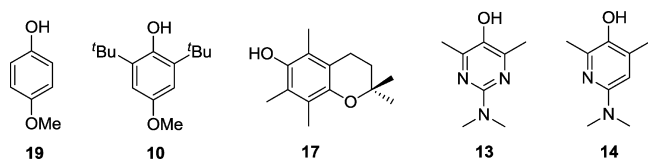
Figure 6. Kinetic isotope effect on the product distribution arising from the decomposition of 3 in the presence of 2,2,5,7,8-pentamethyl-6-chromanol (17) and either 1% D_2O (■) or 1% H_2O (●), which yield $k_H = 5.0 \times 10^6 \text{ M}^{-1} \text{ s}^{-1}$ and $k_D = 2.4 \times 10^6 \text{ M}^{-1} \text{ s}^{-1}$ for $k_H/k_D = 2.1$.

DISCUSSION

Radical clocks based on the carbon-skeleton rearrangements of alkyl radicals have become an indispensable tool in kinetic and mechanistic investigations of reactions where alkyl radicals have been proposed as potential intermediates. Despite the ease with which these types of experiments can be carried out, heteroatom-centered radical clock approaches are few. Among the limited examples are the particularly useful radical clocks based upon competition between the β -fragmentation of a nonconjugated peroxy radical and its reduction to the corresponding hydroperoxide by an H-atom donor, which greatly enables the determination of rate constants for peroxy-molecule reactions.⁸

The first peroxy radical clocks relied on the chain transfer reaction of the antioxidant-derived radical A \cdot with the oxidizable

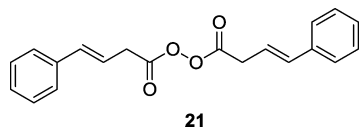
Table 3. Deuterium Kinetic Isotope Effects (k_H/k_D) on the Reactions of a Representative Group of Phenols with Peroxyl Radicals Determined by the Peroxyl Radical Clock Methodology with Peroxyester 3 at 37 °C^a



	k_H/k_D by methodology		
	peroxyester clock (3)	methyl linoleate clock	inhibited autoxidation (ref)
19 ^b	2.5	2.5	n/a
10 ^b	2.2	2.3	n/a
17 ^b	2.1	2.4	5.1 (21)
13 ^c	2.1	1.5	3.1 (16)
14 ^c	1.6	1.5	n/a

^aValues obtained by inhibited autoxidation of styrene and the methyl linoleate-based peroxy radical clock are presented alongside for comparison. ^bObtained in chlorobenzene containing 1% D₂O (or 1% H₂O) as described below. ^cObtained in benzene containing 1% D₂O (or 1% H₂O) as described below.²²

substrate R–H in order to set up the clock (Scheme 1). Since this chain-transfer reaction is quite slow (e.g., 0.1 M⁻¹ s⁻¹ for A· = α -tocopheroxyl and R–H = methyl linoleate,²³ for which $\Delta H \sim 2$ kcal/mol) and will be slowed as A· becomes more stable/persistent and R–H less oxidizable (e.g., allylbenzene, vide supra), this approach is limited. This prompted us to consider other precursors to delocalized radicals that could set up the clock reaction. We first considered diacylperoxides, such as 21, but quickly found that they were simply too labile to be practical.



We next turned to peroxyester 2, which worked nicely as reported in our preliminary communication,⁹ but whose oxidation products often appear in the same part of the (gas) chromatogram as the antioxidant or antioxidant-derived products. We surmised that by replacing the phenyl ring in 2 with a naphthyl ring as in 3, we could push the retention times of the products much later in the chromatogram, improving the resolution and reliability of the analysis. This worked well, with the retention times shifting from ca. 5–10 min on our optimized column/temperature conditions to ca. 12–22 min under the same conditions and, importantly, resolving the expected alcohols and unexpected corresponding carbonyl compounds that were not apparent when 2 was used as precursor to set up the clock (vide infra).

The rate constant for β -fragmentation (k_β) of the non-conjugated peroxy radical derived from 3 was determined in the same way as we did for 2 and was expectedly similar: $k_\beta = 3.0 (\pm 0.9) \times 10^5$ s⁻¹ for the naphthyl analogue compared to $k_\beta = 1.7 (\pm 0.1) \times 10^5$ s⁻¹ for the phenyl analogue⁹ at 37 °C using $k_{inh} = 3.9 \times 10^6$ M⁻¹ s⁻¹ at 37 °C for the standard reaction of α -tocopherol with peroxy radicals in benzene.²⁴ The slight increase in rate constant may reflect the greater delocalization of the allylic radical by the naphthyl π -system as opposed to the

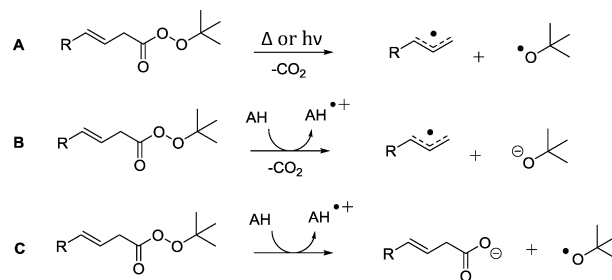
phenyl π -system. Likewise, the oxygen partition coefficient (α) is highly similar: 0.74 ± 0.01 for the naphthyl analogue versus 0.76 ± 0.01 for the phenyl analogue.⁹ This suggested that the clocks could be used essentially interchangeably.

The solvent effects on the β -fragmentation rate constants obtained for the nonconjugated peroxy radical derived from 3 reflect the same trends as those observed for that derived from 2,⁹ although the absolute values vary slightly from solvent to solvent. The overall trend is generally one wherein solvents with greater polarity generally slow the rate of β -fragmentation, consistent with the idea that the peroxy radical is better solvated than the transition state for C–OO· bond dissociation as the polarity of the medium increases.⁹ The oxygen partition coefficients (α) show much higher variance between the two clocks, presumably because of slightly differing orbital interactions of the dioxygen SOMO with the SOMOs of the naphthyl- or phenyl-substituted allyl radicals.^{3,25} Since oxygen partitioning across delocalized carbon-centered radicals is influenced by both sterics and electronics, rationalization of solvent effects on these trends beyond this is difficult.

Nevertheless, with k_β and α defined for a given solvent, the clock can be applied with confidence. We were able to accurately clock reactions of phenols, diarylamines, pyridinols, and pyrimidinols with inhibition rate constants ranging over roughly three orders of magnitude (10^4 – 10^7 M⁻¹ s⁻¹): the range of greatest interest for the assessment of natural products with perceived radical-trapping antioxidant activity and the development of novel synthetic compounds. The rate constants were generally within a factor of 2 or better than literature values obtained using the conventional inhibited autoxidation of styrene methodology.

In carrying out these experiments, we noticed that the amount of products observed in the chromatograms varied with antioxidant. This suggested that the antioxidant was playing a role in the decomposition of the peroxyester. The decomposition of peroxyesters under both photolytic and thermal conditions is well documented (reaction A in Scheme 4). Homolytic cleavage of the weak O–O bond in conjunction with (what is believed to be concerted)²⁶ rupture of the C–C bond results in extrusion of CO₂ and formation of a stabilized allylic radical and a *tert*-butoxyl radical (in the case of 2 or 3). Additionally, peroxyester decomposition can be induced by electron-rich compounds (e.g., dimethylaniline) through donation of an electron into the σ^* orbital of the O–O bond, affording either an acyloxy radical and an alkoxide (B) or a carboxylate anion and an alkoxy radical (C) as shown in Scheme 3.²⁷ Indeed, when the total area of the product peaks

Scheme 3



obtained from clocking experiments at the same concentration of antioxidant ($[ArOH] = 0.06$ M) was plotted as a function of the standard potential of the phenolic antioxidant under study

(E° ranging from 0.12 to 0.9 V²⁸), a linear correlation was obtained (see Figure S2, Supporting Information), supporting induced decomposition of the peroxyester by the antioxidant. Since the clocking experiments are carried out under pseudo-first-order conditions where the antioxidant is in excess, this reaction does not confound our kinetic analysis and serves to improve the yield of products for more reactive (i.e., electron rich) compounds.

In the clocking experiments for compounds 9–14 shown in Table 2, carbonyl products were observed in chromatograms from reactions containing 12–14 but not in those containing 9–11. Since 12–14 each contain basic nitrogen atoms, we surmised that a base-catalyzed dehydration mechanism may be responsible for the formation of these carbonyls.²⁹ Indeed, when mixtures of the conjugated and nonconjugated hydroperoxides 15 and 16 were incubated with varying concentrations of different antioxidants under the same experimental conditions as used in the clocking experiments, the corresponding carbonyl-containing products were observed for those antioxidants containing basic nitrogen atoms. Furthermore, when the solvent was changed from chlorobenzene to acetonitrile, the carbonyl-containing compounds were observed in solutions containing the same additive but in greater yield. When the antioxidant was replaced with triethylamine, the same carbonyl compounds were formed in quantities that correlated with triethylamine concentration. The analogous carbonyl products derived from 2 were not identified in our preliminary report,⁹ presumably because no compounds having sufficient basicity were examined. In fact, when 2 is used to clock these “basic” antioxidants (i.e., 12–14 or 18), cinnamaldehyde (conjugated aldehyde) and 1-phenylprop-2-en-1-one (nonconjugated ketone) are indeed observed as major products in approximately the same ratios as 5 and 7 when peroxyester 3 was used as the clock.

Expectedly, decomposition of 3 at higher temperatures gave rise to higher yields of products. The product ratios were again dependent on α -TOH concentration and could be fit to the kinetics in Scheme 1. The solution of this expression for k_p and α at the higher temperatures required k_{inh} for α -tocopherol at these temperatures. To the best of our knowledge, Arrhenius parameters for the reaction of α -TOH with peroxy radicals are not available, but given the typical $\log A \sim 8$ for H-atom transfer reactions as suggested by Benson³⁰ and the inhibition rate constant for α -TOH in chlorobenzene of $6.4 \times 10^6 \text{ M}^{-1} \text{ s}^{-1}$ at 25 °C,¹⁰ we calculated $E_a = 1.6 \text{ kcal/mol}$ and were able to estimate the k_{inh} at the required temperatures (37, 45, 50, 60, 70, 80, and 95 °C). The resulting Arrhenius plot for the β -fragmentation of the nonconjugated peroxy radical yields $E_a = 9.6 \pm 0.9 \text{ kcal/mol}$ and $\log A = 12.8 \pm 0.6$.³¹ Although these are only estimates, they seem reasonable. The calculated bond dissociation enthalpy (BDE) of the C–OO· bond in the nonconjugated peroxy radical calculated by ROB3P86/6-311G**//UB3P86/6-311G** is 9.8 kcal/mol.³² This method has been shown to give C–OO· BDEs in excellent agreement with experimental values; e.g., for benzylperoxy, the calculated C–OO· BDE value was 22.2 kcal/mol, and it was determined to be $21.8 \pm 0.9 \text{ kcal/mol}$ experimentally.³³ Furthermore, $\log A \sim 13$ for a bond dissociation where a minimum of two bond rotations must be restricted also seems reasonable from first principles.

We anticipate that the use of 3 to measure inhibition rate constants at higher temperatures will be useful in estimating Arrhenius parameters for various phenolic and aromatic amine

antioxidants. There is little of this data in the literature, owing to how difficult it has been to carry out the measurements, and the trends in the limited data available are difficult to understand. For example, while phenol and aniline were found to have $\log A = 7.2 (\pm 0.5)$, $E_a = 5.2 (\pm 0.5) \text{ kcal/mol}$ ³⁴ and $\log A = 6.6 (\pm 0.5)$, $E_a = 5.0 (\pm 0.5) \text{ kcal/mol}$,³⁴ respectively, butylated hydroxytoluene (BHT) and *N*-phenyl- α -naphthylamine were found to have $\log A = 4.2 (\pm 0.3)$, $E_a = 1.4 (\pm 0.3) \text{ kcal/mol}$ ³⁵ and $\log A = 5.1 (\pm 0.5)$, $E_a = 1.0 (\pm 0.4) \text{ kcal/mol}$,³⁵ respectively. The latter result is particularly troublesome given that inhibition rate constants of up to $10^7 \text{ M}^{-1} \text{ s}^{-1}$ have been measured for diarylamines.¹⁵

Deuterium kinetic isotope effects (DKIEs) have long provided direct mechanistic support for H-atom transfer (HAT) or proton-coupled electron transfer (PCET)³⁶ reactions between phenolic and aromatic amine antioxidants and peroxy radicals. Hammond and co-workers originally found very small KIEs for these reactions, leading them to suggest that the mechanism of their chain-breaking activity was due to rate-determining electron transfer followed by a rapid proton transfer.³⁷ Shortly thereafter, Ingold and Howard demonstrated that Hammond's experimental approach had been flawed (protium from product hydroperoxides in inhibited autoxidations could rapidly exchange with the deuterium in the deuterated phenol, precluding the observation of the DKIE) and demonstrated that there was indeed a sizable DKIE in these reactions.²⁰ Since then, DKIEs for the reactions of several phenols with peroxy radicals have been measured by inhibited autoxidation of styrene in the presence of excess D₂O (usually 1% by volume) and generally fall into a range of ~ 3 – 5 in chlorobenzene at ambient temperatures.^{16,21,38}

Utilizing peroxyester 3 (and excess D₂O/H₂O), we obtained highly reproducible primary DKIEs for a representative series of compounds, whose magnitude were roughly half of what were obtained by inhibited autoxidation of styrene where comparison was possible. As an independent check, we measured DKIEs for the same compounds using the first reported peroxy radical clock methodology with methyl linoleate as the oxidizable substrate⁸ and found essentially the same isotope effects as those obtained using the peroxyester approach. The reason for the discrepancy between our measured DKIEs and those obtained using the inhibited autoxidation of styrene method is unclear and under further investigation.

CONCLUSION

β,γ -Unsaturated peroxyesters are convenient and versatile precursors to delocalized radicals for use in peroxy radical clock experiments. In particular, peroxyester 3 yields products that are most conveniently separated by gas chromatography, and resolution of the corresponding alcohol and carbonyl products has allowed us to expand the application of the clock methodology to compounds containing basic moieties with confidence. Additionally, we have demonstrated the utility of peroxyester 3 in measuring deuterium kinetic isotope effects (DKIEs) for a variety of phenolic antioxidants and also discussed its potential in the determination of Arrhenius parameters for peroxy radical-trapping reactions.

EXPERIMENTAL SECTION

Synthesis of (*E*)-*tert*-butyl 4-(naphthalen-2-yl)but-3-eneperoxoate (3). To a suspension of (*E*)-4-(naphthalen-2-yl)but-3-enoic acid (3.00 g, 14.2 mmol) in dry benzene (45 mL) was added SOCl₂ (3.38 g, 28.4 mmol) in one portion. The reaction mixture was heated

at 50 °C until complete as indicated by TLC (ca. 2 h). The solvent was evaporated in vacuo, and the yellow solid obtained was dissolved in dry CH₂Cl₂ (75 mL) and cooled to 0 °C. *tert*-Butyl hydroperoxide (6.7 mL of 5.5 M solution in decane, 36.9 mmol) was then added dropwise, followed by pyridine (freshly distilled over CaH₂, 4.04 g, 51.1 mmol) as a solution in 20 mL of CH₂Cl₂ (dropwise). The reaction was stirred at 0 °C until complete as indicated by TLC (ca. 40 min). The reaction mixture was poured into 50 mL of ice water and extracted with CH₂Cl₂ (2 × 30 mL). The organics were washed with 10% HCl (2 × 20 mL), saturated NaHCO₃ (2 × 20 mL), and brine (20 mL) and dried over MgSO₄. Column chromatography (1:9 Et₂O/petroleum ether) afforded pure product as a white solid. Crystalline product was obtained by recrystallization from ether/hexanes at -20 °C. Yield: 2.67 g (66%); ¹H NMR (CDCl₃, 400 MHz) δ 7.81–7.77 (m, 3H), 7.72 (s, 1H), 7.58 (dd, *J* = 2.0, 4.8 Hz, 1H), 7.49–7.42 (m, 2H), 6.72 (d, *J* = 15.8 Hz, 1H), 6.39 (td, *J* = 7.1, 15.8 Hz, 1H), 3.33 (dd, *J* = 1.4, 7.1 Hz, 2H), 1.35 (s, 9H); ¹³C NMR (CDCl₃, 100 MHz) δ 168.7, 134.3, 133.9, 133.4, 133.0, 128.2, 127.9, 127.6, 126.2, 126.2, 125.9, 123.3, 120.5, 83.6, 35.6, 26.0. HRMS (EI) Calculated: 284.1412. Actual: 284.1451. The starting acid, nonconjugated alcohol **4**,³⁹ nonconjugated ketone **5**,³⁹ conjugated alcohol **6**,⁴⁰ and conjugated aldehyde **7**⁴⁰ were prepared according to literature procedures.

Calibration Experiments. To a screw-capped GC vial was added peroxyester **3** (0.01 M final concentration), α-TOH (**8**) (0.02–1.0 M final concentration), and the desired solvent to a total volume of 100 μL. The samples were incubated for 2–14 h, quenched with 100 μL of 1 M PPh₃, and diluted to 1 mL with acetonitrile for analysis. GC analysis was carried out using an Agilent DB-5 column (30 m × 0.32 μm × 0.25 μm) with the following temperature profile: 130 °C hold 5 min, 2 °C/min to 162 °C, 30 °C/min to 280 °C, hold 5 min. Response factors for the nonconjugated alcohol **4**, nonconjugated ketone **5**, conjugated alcohol **6**, and conjugated aldehyde **7** are 1.85, 1.25, 1.21, and 1.83, respectively, relative to benzyl alcohol. The resulting plot of ([**4**] + [**5**])/([**6**] + [**7**]) vs [α-TOH] was fit using nonlinear regression to obtain *k_β* and *α*.

Clocking Experiments. To a screw-capped GC vial was added peroxyester **3** (0.01 M final concentration), H-atom donor (0.02–1.0 M final concentration depending on *k_{inh}*), and the desired solvent to a total volume of 100 μL. The samples were incubated for 2–14 h, quenched with 100 μL of 1 M PPh₃, and diluted to 1 mL with acetonitrile for analysis. GC analysis was carried out using an Agilent DB-5 column (30 m × 0.32 μm × 0.25 μm) with the following temperature profile: 130 °C hold 5 min, 2 °C/min to 162 °C, 30 °C/min to 280 °C, hold 5 min. A plot of ([**6**] + [**7**])/([**4**] + [**5**]) vs 1/[H-atom donor] was fit linearly to obtain *k_{inh}*. Deuterium kinetic isotope effects were obtained by carrying out measurements in the same manner as above, with the addition of 1% D₂O (or 1% H₂O as a control) to the solvent (after distillation over CaH₂).

■ ASSOCIATED CONTENT

● Supporting Information

Figures S1–S34, all raw data for clock calibration, clocking experiments, temperature-dependence, and isotope effects. This material is available free of charge via the Internet at <http://pubs.acs.org>.

■ AUTHOR INFORMATION

Corresponding Author

*E-mail: dpratt@uottawa.ca.

■ ACKNOWLEDGMENTS

We thank Philip T. Lynett (Queen's University) for measuring deuterium kinetic isotope effects using the methyl linoleate clock methodology and Dr. Luca Valgimigli (University of Bologna) for discussions regarding the Arrhenius parameters for the reactions of phenols with peroxy radicals. We are grateful for the support of the Natural Sciences and

Engineering Research Council of Canada, the Ontario Ministry of Research and Innovation, Queen's University, and the University of Ottawa. D.A.P. also acknowledges the support of the Canada Research Chairs program.

■ REFERENCES

- (1) Ingold, K. U. *Acc. Chem. Res.* **1969**, *2*, 1.
- (2) Porter, N. A. *Acc. Chem. Res.* **1986**, *19*, 262.
- (3) Pratt, D. A.; Porter, N. A.; Tallman, K. A. *Acc. Chem. Res.* **2011**, *44*, 458.
- (4) Ingold, K. U. *Chem. Rev.* **1961**, *61*, 563.
- (5) Mahoney, L. R. *Angew. Chem., Int. Ed.* **1969**, *8*, 547.
- (6) Burton, G. W.; Ingold, K. U. *Acc. Chem. Res.* **1986**, *19*, 194.
- (7) Valgimigli, L.; Pratt, D. A. In *Encyclopedia of Radicals in Chemistry, Biology and Materials*; Chatgillalogu, C., Studer, A., Eds.; Wiley: Hoboken, NJ, 2011.
- (8) Roschek, B.; Tallman, K. A.; Rector, C. L.; Gillmore, J. G.; Pratt, D. A.; Punta, C.; Porter, N. A. *J. Org. Chem.* **2006**, *71*, 3527.
- (9) Jha, M.; Pratt, D. A. *Chem. Commun.* **2008**, 1252.
- (10) Valgimigli, L.; Banks, J. T.; Luszyk, J.; Ingold, K. U. *J. Org. Chem.* **1999**, *64*, 3381.
- (11) When the log *k_{inh}* values for α-TOH obtained by Valgimigli et al. using laser flash photolysis are plotted vs solvent β₂^H, an excellent linear correlation is obtained on which all points reside with the exception of chlorobenzene (see Figure S1, Supporting Information). Since the rate constant obtained in chlorobenzene is almost certainly in error (it is lower than that obtained in benzene, which has a higher β₂^H value), we used the *k_{inh}* value derived from the log *k_{inh}*–β₂^H correlation, which is 6.4 × 10⁶ M⁻¹ s⁻¹ at 25 °C.
- (12) Abraham, M. H.; Grellier, P. L.; Prior, D. V.; Duce, P. P.; Morris, J. J.; Taylor, P. J. *J. Chem. Soc., Perkin Trans.* **1989**, *2*, 699.
- (13) Burton, G. W.; Doba, T.; Gabe, E. J.; Hughes, L.; Lee, F. L.; Prasad, L.; Ingold, K. U. *J. Am. Chem. Soc.* **1985**, *107*, 7053.
- (14) Brownlie, I. T.; Ingold, K. U. *Can. J. Chem.* **1966**, *44*, 861.
- (15) Lucarini, M.; Pedrielli, P.; Pedulli, G. F.; Valgimigli, L.; Gimes, D.; Tordo, P. *J. Am. Chem. Soc.* **1999**, *121*, 11546.
- (16) Pratt, D. A.; DiLabio, G. A.; Brigati, G.; Pedulli, G. F.; Valgimigli, L. *J. Am. Chem. Soc.* **2001**, *123*, 4625.
- (17) Wijtmans, M.; Pratt, D. A.; Valgimigli, L.; DiLabio, G. A.; Pedulli, G. F.; Porter, N. A. *Angew. Chem., Int. Ed.* **2003**, *42*, 4370.
- (18) Bloodworth, A. J.; Curtis, R. J.; Spencer, M. D.; Tallant, N. A. *Tetrahedron* **1993**, *49*, 2729.
- (19) Kornblum, N.; DeLaMare, H. E. *J. Am. Chem. Soc.* **1951**, *73*, 880.
- (20) Ingold, K. U.; Howard, J. A. *Nature* **1962**, *195*, 280.
- (21) Valgimigli, L.; Amorati, R.; Petrucci, S.; Pedulli, G. F.; Hu, D.; Hanthorn, J. J.; Pratt, D. A. *Angew. Chem., Int. Ed.* **2009**, *48*, 8348.
- (22) Russell, G. A. *J. Am. Chem. Soc.* **1957**, *79*, 3871.
- (23) Ingold, K. U.; Bowry, V. W.; Stocker, R.; Walling, C. *Proc. Natl. Acad. Sci. U.S.A.* **1993**, *90*, 45–49.
- (24) To exclude any role of self-association of α-TOH on the determination of *k_β* at the higher concentrations required to accurately calibrate the clock, we also calibrated the clock using 2,6-di-*tert*-butyl-4-methoxyphenol as the H-atom donor (*k_{inh}* = 1.1 × 10⁵ M⁻¹ s⁻¹ at 30 °C in chlorobenzene by the inhibited autoxidation of styrene compared to *k_{inh}* = 3.2 × 10⁶ M⁻¹ s⁻¹ for α-TOH determined by the same investigators under the same conditions)¹³ and found a difference of 3.1-fold on *k_β*. In this case, the double-reciprocal plots were compared for [antioxidant] = 0.02–1.8 M because fitting of the data obtained for 2,6-di-*tert*-butyl-4-methoxyphenol was not possible because of its slower reaction with peroxy radicals.
- (25) Hu, D.; Pratt, D. A. *Chem. Commun.* **2010**, *46*, 3711.
- (26) Bartlett, P. D.; Hiatt, R. R. *J. Am. Chem. Soc.* **1958**, *80*, 1398.
- (27) Antonello, S.; Formaggio, F.; Moretto, A.; Toniolo, C.; Maran, F. *J. Am. Chem. Soc.* **2001**, *123*, 9577.
- (28) Lien, E. J.; Ren, S. J.; Bui, H. Y. H.; Wang, R. B. *Free Radical Biol. Med.* **1999**, *26*, 285.

- (29) Ellam, R. M.; Padbury, J. M. *J. Chem. Soc., Chem. Commun.* **1972**, 1086.
- (30) Benson, S. W. *Thermochemical Kinetics*, 2nd ed.; John Wiley & Sons: New York, 1976.
- (31) If $\log A = 7.5$ is used for the reaction of α -TOH with peroxy radicals, $\log A$ and E_a for the β -fragmentation of the nonconjugated peroxy radical become 12.3 and 8.9 kcal/mol, respectively. Similarly, if $\log A = 8.5$ is used for the reaction of α -TOH with peroxy radicals, $\log A$ and E_a for the β -fragmentation of the nonconjugated peroxy radical become 13.3 and 10.3 kcal/mol, respectively.
- (32) DiLabio, G. A.; Pratt, D. A. *J. Phys. Chem. A* **2000**, *104*, 1938.
- (33) Fenter, F. F.; Noziere, B.; Carlap, P.; Lesclaux, R. *Int. J. Chem. Kinet.* **1994**, *26*, 171.
- (34) Chenier, J. H. B.; Furimsky, E.; Howard, J. A. *Can. J. Chem.* **1974**, *52*, 3682.
- (35) Howard, J. A.; Furimsky, E. *Can. J. Chem.* **1973**, *51*, 3738.
- (36) Litwinienko, G.; Ingold, K. U. *Acc. Chem. Res.* **2007**, *40*, 222.
- (37) Hammond, G. S.; Boozer, C. E.; Hamilton, C. E.; Sen, J. N. *J. Am. Chem. Soc.* **1955**, *77*, 3238.
- (38) Burton, G. W.; Ingold, K. U. *J. Am. Chem. Soc.* **1981**, *103*, 6472.
- (39) Brigham & Women's Hospital.; Augelli Szafran, C. E.; Wolfe, M. S.; Han Xun, W.; European Patent Office, 2009, WO2008US11649 20081010.
- (40) Avery, T. D.; Caiazza, D.; Culbert, J. A.; Taylor, D. K.; Tiekink, E. R. T. *J. Org. Chem.* **2005**, *70*, 8344.